26 February 1999

ELSEVIER

Chemical Physics Letters 301 (1999) 372–378

CHEMICAL PHYSICS LETTERS

Crossed-beam reaction of $O(^1D) + D_2 \rightarrow OD + D$ by velocity map imaging

Musahid Ahmed, Darcy S. Peterka, Arthur G. Suits *

Chemical Sciences Division, Ernest Orlando Lawrence Berkeley National Laboratory, Berkeley, CA 94720, USA

Received 5 November 1998; in final form 5 January 1999

Abstract

The technique of velocity map imaging [Eppink and Parker, Rev. Sci. Instrum. 68 (1997) 3477] has been applied to the reaction $O(^1D) + D_2 \rightarrow OD + D$ under single-collision conditions in crossed molecular beams at a collision energy (E_{coll}) of 2.4 kcal/mol. Images of the reactively scattered D-atom product were recorded, yielding the full double differential cross-sections (energy and angle) for the reaction. The translational energy and angular distributions are observed to be strongly coupled, with the forward-scattered products showing the largest translational energy release and the sideways-scattered products the lowest translational energy release.

1. Introduction

The reaction $O(^1D)$ with molecular hydrogen and its isotopic variants has long been considered a prototypical insertion reaction, with most collisions at thermal energies believed to access the region of the deep H_2O well [1]. An early crossed molecular beam study found forward–backward symmetry in the angular distribution for collision at 2.7 kcal/mol [2]. This was ascribed to an insertion reaction mechanism, with symmetry in the decaying intermediate invoked to account for the angular distribution. Trajectory calculations [3–7] and a quantum reactive scattering study with reduced dimensionality [8] have, in the past, consistently shown forward–backward symmetric angular distributions and thus the importance of the insertion mechanism. However, recent work [1], both theoretical and experimental, has begun to challenge this notion of simple insertion on the ground electronic potential energy surface (PES).

Che and Liu, using a conventional Doppler-shift technique in conjunction with crossed molecular beams, observed enhanced backward scattering for collisions of $O(^1D)$ with HD at 4.55 kcal/mol [10]. Hsu and Liu confirmed this observation very recently using a high-resolution Doppler-selected time-of-flight (TOF) method [11]. They were also able to see some structure in the energy distributions at different angles which they believed correlated to vibrational–rotational states of the corresponding OH/OD product. Subsequently Ho et al. carried out trajectory calculations based on a new global PES

* Corresponding author. E-mail: agsuits@lbl.gov; fax: +1 510 486 5664

[1] For a general discussion on the role of excited states see Ref. [9].

0009-2614/99/$ - see front matter
PII: S0009-2614(99)00048-2

[12]. Their results support the insertion mechanism with a short-lived complex, and they could not reproduce the strong preference for backward scattering seen in the work of Che and Liu. Alexander et al. have also performed QCT calculations on the $O(^1D) + HD$ reaction [13]. Their results agreed with the translational energy distributions ($P(E_T)$) extracted from the earlier experiment of Che and Liu, but their state-averaged angular distribution showed forward–backward symmetry. Alexander et al. also studied the $O(^1D) + H_2$ reaction using polarized Doppler-resolved laser spectroscopy to probe the product state-resolved differential cross-section under bulb conditions [14,15]. They found sharply peaked backward scattering in the channel generating OH ($v = 0$, $N = 5$) and forward–backward scattering for OH ($v = 0$, $N = 14$) but their collision energy was not well defined.

Alagia et al. [16], very recently, reported their results on the title reaction using crossed molecular beams with universal detection. They found nearly backward–forward symmetric angular distributions with a favored backward peaking which increased with collision energy. They also performed QCT calculations using a single surface and found poor agreement with the experimental results. Schatz et al. [17,18] have performed a series of QCT calculations with an eye on studying the excited-state dynamics of this reaction. They found that the inclusion of the first excited state gives rise to predominantly backward scattering, and their theoretical results qualitatively agree with the results of Alagia et al. for $O(^1D) + D_2$ at $E_{coll} = 5.3$ kcal/mol and with those of Hsu and Liu for $O(^1D) + HD$ at $E_{coll} = 4.53$ kcal/mol.

We have begun an in-depth experimental study to explore the role of excited-state dynamics using the ion-imaging technique in crossed molecular beams. Ion imaging is a multiplexing method which provides simultaneous detection of all recoil velocities, both speed and angle, for the detected product. One of the most appealing factors is the very direct way the raw data presents itself to the experimenter. Further, the images may be directly deconvoluted to yield the velocity-flux contour maps which summarize the dynamics. The deconvolution does not require the simplifying assumption of uncoupled translational energy and angular distributions usually employed in analyzing reactive scattering experiments. The imaging experiments thus directly reveal the genuine double differential cross-sections ($d^2\sigma / dE_T\, d(\cos\theta)$), a particularly important feature in the $O(^1D) + D_2$ reaction.

To date, there have been two scattering experiments performed with traditional ion-imaging techniques: inelastic scattering of Ar–NO [19] and reactive scattering [20] of $H + D_2$. In the past, the ion-imaging technique suffered from limited velocity and angular resolution, largely determined by the dimensions of the interaction region relative to the detector and by blurring from lensing effects associated with the grids. A recent advance by Eppink and Parker [21] involves simply replacing the conventional grids of the Wiley–McLaren TOF spectrometer with open electrostatic lenses and adjusting the potentials to achieve momentum focusing. Under these conditions, termed 'velocity map imaging' (VELMI), all products with the same initial velocity vector in the plane parallel to the detector are focused to the same point, irrespective of their initial distance from the ion lens axis.

2. Experimental

The crossed molecular beams apparatus (Fig. 1) has been described in detail in a recent publication [22]. The $O(^1D)$ beam was generated by photodissociation of O_3 seeded in He, using the 266 nm output of a Nd:YAG laser (Spectra-Physics GCR 290-30), at the nozzle of a Proch–Trickl piezoelectric pulsed valve [23]. The molecular beam of ozone was generated by passing helium through ozone trapped on silica gel, held at -40°C. After the beam was collimated by a skimmer, it was chopped by means of a rotating slotted wheel (200 Hz; diameter, 17.8 cm; width, 1 mm), to generate a short rectangular pulse (7.5 μs) of $O(^1D)$. The O-atom beam velocity and spread were monitored using either (2 + 1) REMPI of $O(^1D)$ or, conveniently, vacuum–ultraviolet (VUV) photoionization of the O_2 co-photo fragment (using the same light used to probe the reactively scattered D-atom product). Neat D_2 was expanded through another Prock–Trickl pulsed valve, collimated by a single skimmer and the beams were allowed to interact on the axis of the velocity focus-

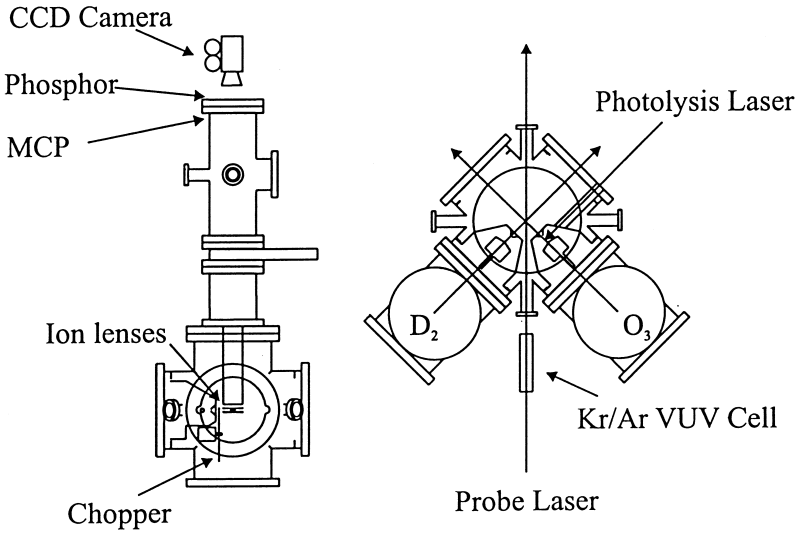

Fig. 1. Schematic view of the experimental apparatus.

ing TOF mass spectrometer. We estimate the rotational temperature of the D_2 beam to be less than 5 K.

The product D-atoms were ionized using a two color $(1+1)$ ($\lambda = 121.6$ and 212.5 nm) REMPI scheme. The VUV Lyman-α light was generated by difference frequency mixing [24] of ultraviolet (UV) and infrared (IR) light in krypton, phase matched with argon. The UV light (212.5 nm, a two-photon resonance in Kr) was generated by doubling the output of a seeded Nd:YAG (Spectra-Physics GCR 290-30) pumped dye laser (Laser Analytical Systems LDL) operating at 637.5 nm in β-barium borate (BBO), then mixing the resultant UV light with the dye fundamental in a second BBO crystal. The polarization of the UV and visible beams were corrected using a waveplate before mixing. Infrared light around 840 nm was generated using a second Nd:YAG pumped dye laser (Laser Analytical Systems LDL), and the two beams were collimated using a dichroic mirror and focused into the rare-gas cell. The resultant VUV output was loosely focused into the interaction region of the molecular beams using a MgF_2 lens.

The D^+ ion was accelerated toward a 40 mm diameter dual microchannel plate (MCP) (Galileo 3040FM) coupled to a fast phosphor screen (P-47) and imaged on a fast-scan charge-coupled device camera with integrating video recorder (Data Design AC-101M). Camera threshold and gain were adjusted in conjunction with a binary video look-up table to perform integration of single ion hits on the MCP free of video noise. Images were accumulated while scanning across the Doppler profile of the D-atom, since the line width of the laser light was narrower than the Doppler spread. The recorded image is actually a 2-dimensional (2-D) projection of the nascent 3-dimensional (3-D) velocity distribution, and established tomographic techniques were used to reconstruct the 3-D distribution [25]. Typical accumulation time for a single-collision energy was about 120 min. A background image obtained with the photolyis laser off was subtracted from the raw data image, but this represented a minor correction.

One difference between conventional imaging and velocity mapping is the necessity in the latter case to calibrate the magnification of the image. In these studies, calibration was conveniently performed using the known velocity of room-temperature beams, since the VUV probe was generated using a Kr resonance. This calibration was confirmed by performing photodissociation studies of H_2S and CH_4 and detecting the H-atom product.

An important question in crossed-beam studies using pulsed beams and laser probe concerns the speed dependence of the detection probability and

the influence of the relative sizes of the interaction and probe volumes. In order to understand these influences, the experiment was simulated using a Monte Carlo forward convolution program [26]. This program was found to yield accurate analyses of crossed-beam imaging data in previous Ar–NO scattering studies [27]. In this simulation, limiting cases of the relative sizes of the probe and interaction volumes were considered, with the known experimental conditions (e.g., beam velocity and angular distributions) used to determine the detection probability as a function of D-atom recoil speed or translational energy. The slow fragments are detected much more efficiently than the fast products regardless of the relative sizes of the probe and interaction volume. This is owing to the finite duration of the molecular beam pulses relative to the probe laser. Significant contributions were found for scattering events up to 0.5 μs before arrival of the probe pulse. Results reported below were thus scaled according to these detection efficiencies. Although this represents a substantial correction to the product velocity distributions, the relative insensitivity of the detection efficiency to the size of the probe volume gives us confidence in applying this correction.

3. Results and discussion

Fig. 2A shows a raw image of D-atoms recorded using the VELMI technique. Seven separate images were blended together to generate the composite image shown. The relative velocity vector is vertical in the plane of the figure, and the Newton diagram for the scattering process has been superimposed on the image. Fig. 2B shows a detailed schematic of the same Newton diagram. The dominant feature is the broader distribution of the fast back-scattered D-atom (relative to the incoming D_2 beam), the sharper peaking distribution of the fast forward-scattered products, and the overall slower sideways-scattered products, giving rise to an 'arrowhead' shape of the image. This self-evident nature of the distributions in these images underscores the power of the technique to yield the double differential cross-sections directly.

The cylindrical symmetry of the experiment justifies the use of the inverse Abel transform method to

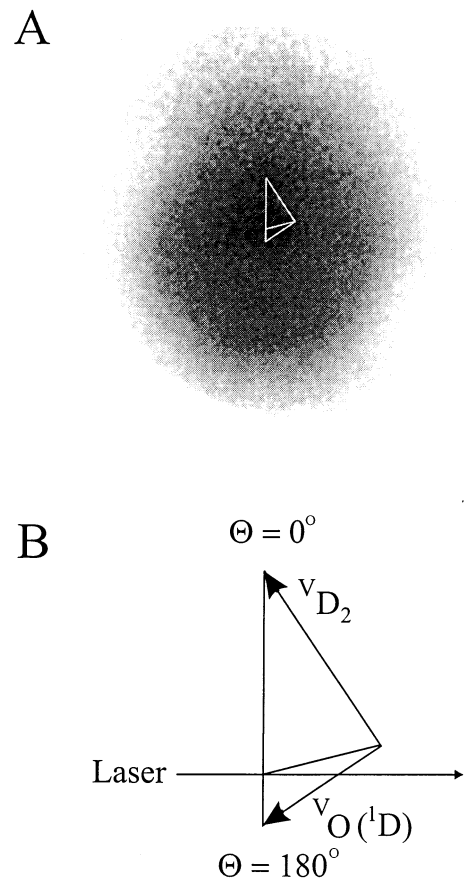

Fig. 2. (A) Image of D-atoms formed in the reaction of $O(^1D) + D_2$ at a collision energy of 2.4 kcal/mol using velocity map imaging. The Newton diagram is superimposed on the image, and a detailed expanded version is shown in Fig. 2 (B).

reconstruct the full 3-D distributions, so that this analysis is, in effect, a direct inversion of the experimental data. The cm angular distributions $[d\sigma/d(\theta)]$, extracted from the images are shown in Fig. 3. The distribution is peaked sharply in the forward direction and is broader in the backward direction as is apparent from the raw data. The distribution at the poles are 2.75 (forward) and 2.25 (backward) times larger than at the equator. However the total cm angular distribution does not reveal the subtleties inherent in the differential cross-section. A revealing way to look at the detailed dynamics of this system is to display the angular distributions for different segments of the translational energy distributions. Fig. 4 show the angular distributions for four regions

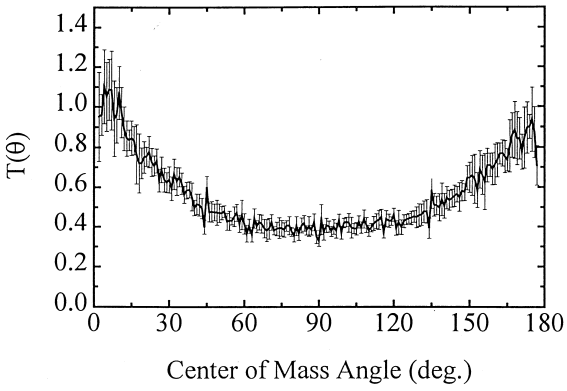

Fig. 3. Center-of-mass angular distributions obtained from the Abel-transformed image for $E_{coll} = 2.4$ kcal/mol. The direction of the D_2 and $O(^1D)$ beams correspond to 0° and 180°, respectively. The error bars represent the standard deviation from results for seven separate images.

of the translational energy distributions. At low translational energy release the distribution is symmetric; with an increase in translational energy the distributions are sharply peaked in the forward direction and broad in the backward direction. Fig. 5 shows the translation energy distributions obtained from the reconstructed data for four distinct regions of angular recoil (from 0° to 180°, in 45° increments). At $E_{coll} = 2.4$ kcal/mol, the forward component peaks at lower translation energy, ~ 8 kcal/mol, and extends beyond our detection capability, while the backward portion peaks at about ~ 11 kcal/mol and drops sharply beyond 30 kcal/mol. The sideways component peaks at about ~ 10 kcal/mol, but then drops sharply beyond 20 kcal/mol. Very similar translational energy distributions were reported by Hsu and Liu [11] for the D-atom from the $O(^1D) + HD$ reaction at $E_{coll} = 4.53$ kcal/mol using the Doppler-selected TOF technique.

The comparison between our results and those of other studies of this reaction highlights the relative advantages and disadvantages of the various techniques. In the present work, we have confined ourselves to the dynamics at a single-collision energy, below that at which excited-state contributions have been invoked. In the future we plan to extend these studies to higher collision energies to probe directly for excited-state contributions to the dynamics. Recent work from the Perugia group [16] using the conventional crossed-beam method are globally similar to ours but show important differences. Their results were fitted with a single uncoupled angular

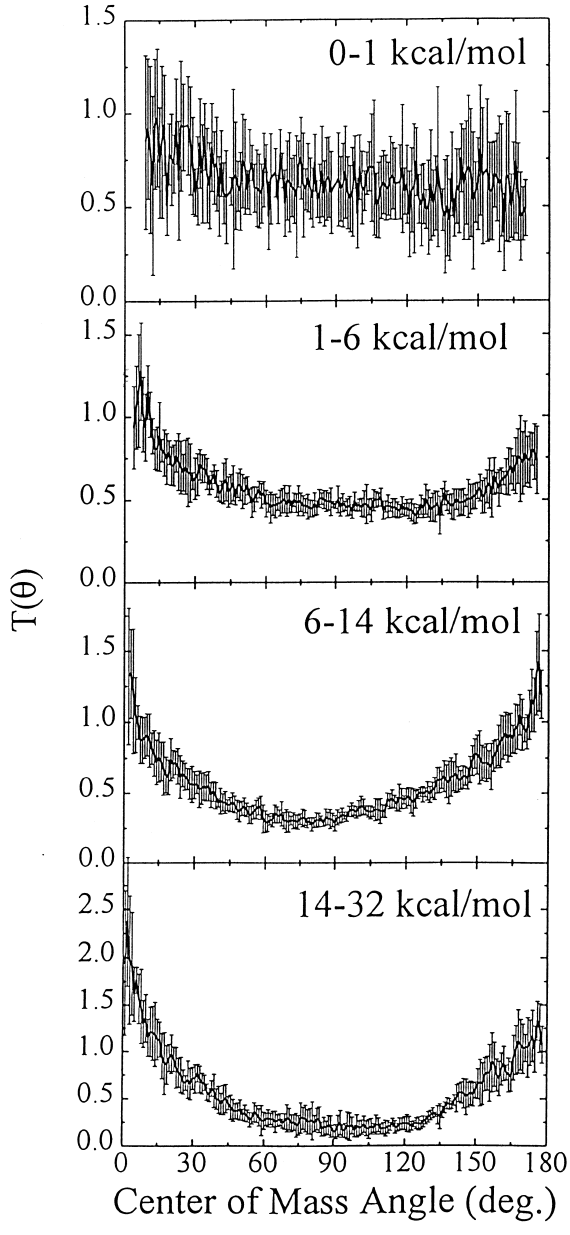

Fig. 4. Center-of-mass angular distributions obtained for a range of translational energy release. The direction of the D_2 and $O(^1D)$ beams correspond to 0° and 180°, respectively. The error bars represent the standard deviation obtained for each point from seven separate images.

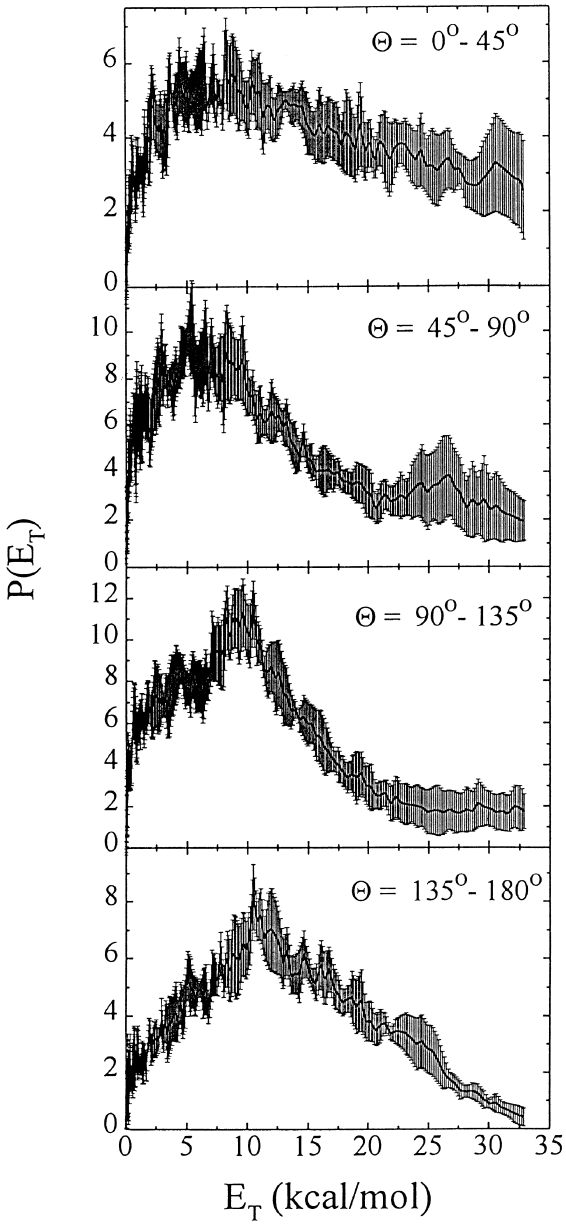

Fig. 5. Total translational energy (E_T) distributions obtained from Abel-transformed images for four distinct regions of angular recoil. The error bars represent the standard deviation obtained for each point from seven separate images.

and translational energy distribution; our results show unambiguously that there is strong coupling between the two. In this respect our results agree well with Hsu and Liu [11]. The low translational energy component of our distributions, particularly in the backscattered direction, do not rise as quickly as those of Alagia et al. [16], again our results agree better with the Hsu and Liu here. However, the Perugia experiments are particularly sensitive to this portion of the distribution since the lab-cm transformation Jacobian exaggerates the contribution of the slow products in the traditional crossed-beam experiments; their results may well be more reliable at the lowest translational energies. The elegant Doppler-resolved ion TOF experiment of Hsu and Liu involves both an inversion of the data and a transformation from the Cartesian system in which the experiment is performed to the polar scattering frame, again making the direct connection to the experiment somewhat elusive. For the sideways-scattered component, the results of Hsu and Liu show extraordinary resolution. Unfortunately the resolution of that method is a complicated function of scattering angle and recoil velocity, and the resolution in the portion of the distribution scattered to the poles is limited. The results of Simons and co-workers [14,15,28] for the H_2 reaction obtained using a state-resolved Doppler probe under room temperature bulb conditions are difficult to compare directly to the crossed-beam experiments. Alexander et al. [28] have only reported results for a few product rotational levels; moreover their collision energy is very broad. Nevertheless, they extract excitation functions for the detected state on the basis of an assumed separability of the translational and angular distributions. With this assumption, and probe of OH($v = 4$, $N = 1$), they see no evidence for an excited-state contribution which has been invoked by the other groups [11,16] to explain the experimental results.

These results represent the first application of the powerful VELMI technique to a bimolecular reaction, and show the potential of the method to reveal details of reactive processes. In this case, the application of the VELMI technique to the widely studied $O(^1D)$ + hydrogen reaction showcases its ability to expose the detailed coupling of the translational energy and angular distributions that are key to understanding the dynamics. In addition, as this reaction has been aggressively studied recently in several laboratories using alternative methods, it provides a unique opportunity to examine the strengths and weaknesses of each method.

Acknowledgements

The authors gratefully acknowledge G. Schatz, K. Liu, and P. Casavecchia for valuable discussions and comments, and K. Liu, G. Schatz, D. Parker, P. Casavecchia and P.J. Knowles for providing preprints of their most recent work. AGS would like to thank D. Chandler and the Sandia Combustion Research Facility for hosting a workshop on imaging methods at which the velocity mapping technique was discussed. This work was supported by the Director, Office of Energy Research, Office of Basic Energy Sciences, Chemical Sciences Division of the US Department of Energy under Contract No. DEACO3-76SF00098.

References

[1] R.D. Levine, R.B. Bernstein, Molecular Reaction Dynamics and Chemical Reactivity, Oxford University, New York, 1987.
[2] R.J. Buss, P. Casavecchia, T. Hirooka, S.J. Sibener, Y.T. Lee, Chem. Phys. Lett. 82 (1981) 386.
[3] K.S. Sorbie, J.N. Murrell, Mol. Phys. 31 (1976) 905.
[4] R. Schinke, W.A. Lester Jr., J. Chem. Phys. 72 (1980) 3754.
[5] S.W. Ransome, J.S. Wright, J. Chem. Phys. 77 (1982) 6346.
[6] P.A. Whitlock, J.T. Muckerman, E.R. Fisher, J. Chem. Phys. 76 (1982) 4468.
[7] L.J. Dunne, J.N. Murrell, Mol. Phys. 50 (1983) 635.
[8] J.K. Badenhoop, H. Koizumi, G.C. Schatz, J. Chem. Phys. 91 (1989) 142.
[9] R. Donovan, G.C. Schatz, M. Alexander, R.B. Gerber, S. Mohr, K.M. Goonan, R. Grice, P. Casavecchia, M. Janssen, J.P. Simons, M.N.R. Ashfold, A. Suits, P.J. Dagdigian, K. McKendrick, G. BalintKurti, T. Minton, V.A. Apkarian, M. Gonzalez, J.P. Visticot, J.C. Polanyi, T. Moller, C. Whitehead, R. Grice, G. Scoles, B. Soep, A. Hudson, D. Neumark, R.E. Continetti, S.R. Langford, J. Jortner, Faraday Disc. 108 (1997) 427.
[10] D.-C. Che, K. Liu, J. Chem. Phys. 103 (1995) 5164.
[11] Y.-T. Hsu, K. Liu, J. Chem. Phys. 107 (1997) 1664.
[12] T.-S. Ho, T. Hollebeek, H. Rabitz, L.B. Harding, G.C. Schatz, J. Chem. Phys. 105 (1996) 10472.
[13] A.J. Alexander, F.J. Aoiz, M. Brouard, J.P. Simons, Chem. Phys. Lett. 256 (1996) 561.
[14] A.J. Alexander, F.J. Aoiz, M. Brouard, I. Burak, Y. Fujimura, J. Short, J.P. Simons, Chem. Phys. Lett. 262 (1996) 589.
[15] A.J. Alexander, F.J. Aoiz, L. Banares, M. Brouard, J. Short, J.P. Simons, J. Phys. Chem. A 101 (1997) 7544.
[16] M. Alagia, N. Balucani, L. Cartechini, P. Casavecchia, E.H. van Kleef, G.G. Volpi, P.J. Kuntz, J.J. Sloan, J. Chem. Phys. 108 (1998) 6698.
[17] G.C. Schatz, A. Papaioannou, L. Pederson, L.B. Harding, T. Hollebeek, T.-S. Ho, H. Rabitz, J. Chem. Phys. 107 (1997) 2340.
[18] G.C. Schatz, L.A. Pederson, P.J. Kuntz, Faraday Disc. 108 (1997) 357.
[19] A.G. Suits, L.J. Bontuyan, P.L. Houston, B.J. Whitaker, J. Chem. Phys. 96 (1992) 8618.
[20] T.A. Kitsopoulos, D.P. Baldwin, M.A. Buntine, R.N. Zare, D.W. Chandler, Science 260 (1993) 1605.
[21] A.T.J.B. Eppink, D.H. Parker, Rev. Sci. Instrum. 68 (1997) 3477.
[22] M. Ahmed, D. Blunt, D. Chen, A.G. Suits, J. Chem. Phys. 106 (1997) 7617.
[23] D. Proch, T. Trickl, Rev. Sci. Instrum. 60 (1989) 713.
[24] G. Hilber, A. Lago, R. Wallenstein, J. Opt. Soc. Am. B 4 (1987) 1753.
[25] B.J. Whitaker, in: R.G. Compton, G. Hancock (Eds.), Research in Chemical Kinetics, Vol. 1, Elsevier, Amsterdam, 1993.
[26] L.S. Bontuyan, A.G. Suits, P.L. Houston, B.J. Whitaker, J. Phys. Chem. 97 (1993) 6342.
[27] S.D. Jons, J.E. Shirley, M.T. Vonk, C.F. Giese, W.R. Gentry, J. Chem. Phys. 97 (1992) 7831.
[28] A.J. Alexander, D.A. Blunt, M. Brouard, J.P. Simons, F.J. Aoiz, L. Banares, Y. Fujimura, M. Tsubouchi, Faraday Disc. 108 (1997) 375.